Folding Propeller Design and Analysis for a Hybrid Driven Underwater Glider

Zhier Chen[1,2]
1.University of Chinese Academy of Sciences
Beijing, China
2. Shenyang Institute of Automation, Chinese Academy of Sciences
Shenyang, China
chenze@sia.cn

Jiancheng Yu,Aiqun Zhang,Ruiwen Yi,Qifeng Zhang
Shenyang Institute of Automation, Chinese Academy of Sciences
Shenyang, China

Abstract*—This paper designed a folding propulsion module dedicated for a hybrid driven underwater glider (HDUG). The blades of the propulsion module can be folded and unfolded in time when a mission needed. In this paper, the design of the driven device and its hydrodynamic performance analysis are described respectively. we used the spline curves to fit the individual data points, base on which we created a three dimensional solid model of an unfolding propeller having smooth surfaces after drawing the profile shape line based on the coordinate transformation. CFD method was used to calculate the performance of the folding propeller in the viscous flow regions with various blade opening angles from 0 to 90 degrees. The thrust coefficient, torque coefficient and propulsive efficiency of the folding propeller have been simulated under different advance coefficients and different blade opening angles. For the purpose of evaluate the degree of drag decrease, we proposed a conception of drag decrease fraction. We obtained the drag decrease fraction of the whole vehicle reached to 45% compared the blades in folding and unfolding. Finally, we gave a result analysis and discussion and found out that the design of the propulsion module meet the requirements well when the motor speed is greater than 800 revolutions per minute.

Keywords—propeller; hydrodynamic; underwater glider; hybrid driven; folding

I. INTRODUCTION

In the past ten years, autonomous underwater glider (AUG) is widely used in oceanographic research [1-4]. The buoyancy control system, the focus adjustment system, and the hydrodynamic components such as a pair of fixed wings help an AUG navigate in the horizontal or vertical cross-section direction to complete a zigzag path[5-8]. Usually the endurance capacity of this kind of vehicle can reach a few months, especially for thermal Glider with higher endurance[7]. In comparison, the current autonomous underwater vehicle (AUV) has much lower endurance. In addition, the velocity of most AUGs is lower than AUVs, especially in the strong flow of water and if the velocity of flow exceeds the maximum speed of AUG's then this can have significant impact on AUG's controllability. In one hand, when AUG works in this kind of environment, we can effectively plan a path for the vehicle according to a mission requirement if the ocean parameters such as the current velocity and direction are known or can be real-time monitored[9, 10]. In other hand, if the environment parameters are unknown, there may be have risks in our successful implementation of the task. Thirdly, the saw-tooth-path characteristic is unable to maintain a horizontal posture sailing which greatly limited the AUG's continuous operation in the horizontal plane and other marine science applications. These issues bring us an idea that we can combine the characteristics of traditional AUG's buoyancy system with the AUV's propeller system to develop a hybrid driven underwater glider (HDUG). References [11-15]list some HDUGs researched by many countries around the world. HDUG's mechanism of implementation is based on the existing small AUV and AUG. This paper also does some research on HDUG, focusing on solving the driven device implementation issues. Currently most of the driven devices of HDUG around the world are based on propeller and water jet. The most important feature of the HDUG in this study is a stern driven module based on a new type of folding propeller (shows in Fig.1).

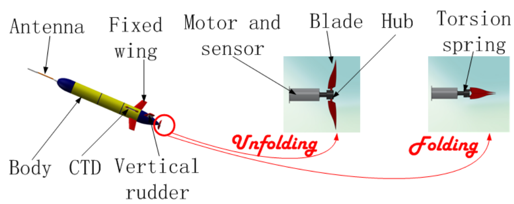

Fig. 1. Model of HDUG and the folding propeller

The HDUG is able to not only move in horizontal plane using propeller driven (AUV mode) but also glide in vertical plane with buoyancy driven (Glider mode); Furthermore the HDUG owns the ability to move with the former two modes at the same time (AUV/Glider mixed mode) which is different from others. Controllable parameters corresponding to the three modes are shown in Fig.2, where υ represents the speed of the HDUG, ΔB represents the net buoyancy, Ω represents the desired motor speed.

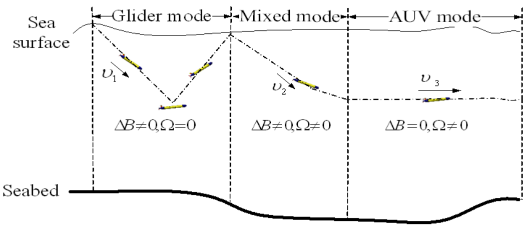

Fig. 2. Three driven modes of the HDUG

978-0-933957-40-4 ©2013 MTS

This folding propeller module is a new type of driven device whose blades can be folded or unfolded depending on the task demands, thus the hydrodynamic resistance of the HDUG can be reduced when blades are folded. Folding propeller device has been widely used in sailboat. The actual results show that this device greatly helps athletes to improve their performance. However, due to the small volume of underwater vehicles such as AUV or AUG, the folding propeller device must be small, light, and complex resulting in more difficult to achieve. In 2009, Brian Claus had used an aerostatic folding propeller on AUG. However, the propeller efficiency is not high[12].

This paper developed a foldable propeller driven module dedicated to HDUG, which has the following characteristics:

- The module is small in size, light in weight, simple in principle.
- Blade reset mechanism is simple using torque spring, no extra energy consumption needed.
- The module has a good performance in hydrodynamic.
- The module has a blade position detection function. This function can timely detect whether the blade-closed-surface is in an vertical position and correct it if not. The reason for keeping the blade-closed-surface in vertical position is to reduce the impact of hydrodynamic performance of blades on the HDUG, which is illustrated in Fig.3.

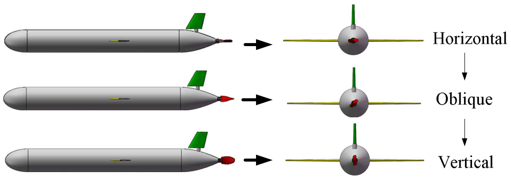

Fig. 3. Different blade-closed-surface position

This module enables the HDUG to glide at 0.5 knot in vertical plane, and move at 2 knots in horizontal plane in a short time. In addition, the HDUG can glide at a speed higher than the traditional AUG with the hybrid driven mode. The driven module works as follows: The blades of the module can be unfolded through the centrifugal force with the motor high speed rotation then produce thrust required by the HDUG movement; The blades can be folded by the hydrodynamic resistance and the internal reset spring mechanism (shows in Fig.1). The key issues of the HDUG's dedicated folding propeller driven device include the propeller hydrodynamic performance, realization of the blades folded and unfolded, blade position detection, low resistance performance optimization, matching among the vehicle body, the motor, and the propeller. The propeller hydrodynamic performance of the driven unit is one of the key problems. This paper will discuss this problem.

Propeller hydrodynamic performance obtained from experiments in open water[16]. The results can be used as reference variables to build dynamics and kinematics equations for the HDUG. Therefore, open water performance numerical calculation is important to study the HDUG. CFD numerical simulation experiments have advantages of more adaptability, wide range of applications, and short cycle compared with physical tests. Firstly, most fluid problems whose equations are nonlinear and have lots of variables. In addition, the computational domains are arbitrary and the boundary conditions are complicated. These issues may lead to unable to obtain an analytical solution. However, the numerical solution can well meet the needs of these engineering problems. Secondly, we can use a computer to do many numerical experiments. We can select different parameters to improve the calculation results. Thirdly, the numerical simulations can be carried out when the physical model is unprocessed. The results can be used as a basis for modifying the model, thus we can avoid waste of resources. Therefore, we use numerical calculation method to simulate the open water experiments of the folding propeller driven module. The blades are the most critical parts to determine the hydrodynamic performance of the module. Therefore, we simplify the mathematical model of the folding propeller device, leaving only the blades and the hub, and conduct open water experiments.

II. The Designed Folding Propeller Model

A. Main Structural Component

The designed folding propeller driven module dedicated for HDUG includes: a driven motor, a blade position detecting device, a reset device (torsion springs), two blades, and a hub, which is shown in Fig.4.

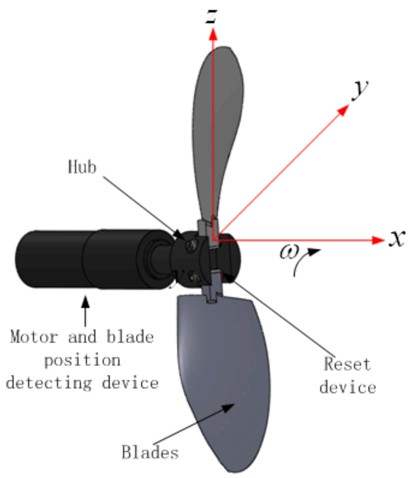

Fig. 4. Main structural component of the designed folding propeller driven module

B. Physical Geometry of Parametric

The number of propeller blades is usually selected as two or more. Generally, if the diameter and the expanded area of the blades are the same size, then the propeller of which number of blades is less has higher efficiency. Because the propeller efficiency will be reduced as a result of increasing cascade interference with the blades grow in number. In addition, a small number of blades is good for the propeller to avoid cavitations[16]. Therefore, this paper presents a two blades folding propeller according to estimates of hydrodynamic resistance and some other key parameters of Sea-wing glider in Shenyang Institute of Automation, Chinese Academy of Sciences[17]. The physical geometry parameters of the folding propeller are shown in the following table in which A_E is the expanded area, and A_O is the disc area.

TABLE I. PROPELLER'S PHYSICAL GEOMETRY OF PARAMETRIC

Propeller Diameter, D	0.28m
Pitch/propeller diameter ratio , P/D	0.786
Hub/ propeller diameter ratio, d_h/D	0.04
Material of blades	ABS
Single blade weight, m	0.022kg
Number of blades	2
Material of hub	2024metal
Hub weight, m_h	0.090kg
Spring wire diameter, d_1	1mm
Spring in diameter , d_2	8mm
Spring material	Silicon bronze wire
Modulus of elasticity , E	93.2 GP_a
Number of active coils of the spring, N	4
Number of springs of each blade, Z	2

C. The Realization of Blade's Folded and Unfolded

The folding propeller driven module dedicated for HDUG has a complex internal structure due to its small volume. Especially in Glider mode, since the forward velocity of the HDUG is slow, the pressure of the water is not enough to fold the blades. Therefore, the blades must be folded by means of the reset mechanism which is different from others. Wherefore it is necessary to analyze the implement mechanism of the entire apparatus specially.

1) Blades Unfolding:

The propeller rotates with the motor rotating when the HDUG need to enter the AUV mode or AUV / Glider mixed mode. At this point the propeller blades are gradually unfolded under the action of centrifugal force and hydrodynamic. The folding angle θ is from 0° gradually approaching 90° .Finally the propeller blades achieve dynamic torque balance under the action of centrifugal force, hydrodynamic thrust, torsion spring force and gravity. A moving coordinate system (o-xyz) with origin (o) which is the midpoint of the blade rotation axis was built in Fig.4 and Fig.5. Where positive of axis x parallels to the central axis of hub and points to the stern of the HDUG; Positive of axis z is upright; Axis y parallels to the axis of blade rotation. We can obtain a new coordinate system o'-$x'y'z$ by translate the coordinate system o-xyz along the z-axis negative direction for r length. Where r is the distance between the rotation axis of the blade and the hub. In this paper, r = 0.01m (see Fig.5 (a)).

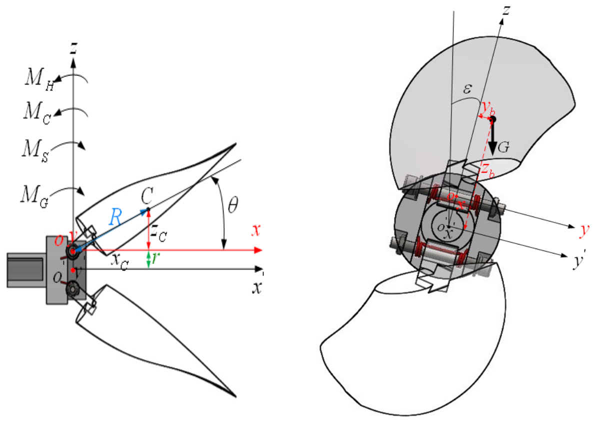

(a) xoz plane (b) yoz plane

Fig. 5. Blade moment equilibrium analysis

According to the moment equilibrium relations, we get the function:

$$-M_C^y - M_H^y + M_S^y + M_G^y = 0 \tag{1}$$

Here, M_C^y is the centrifugal moment acting on the blade relative to the y-axis component with unit $N \bullet m$. We take an element of mass dm of which the barycentric coordinate is (x_{c0}, y_{c0}, z_{c0}). M_C^y can be calculated by:

$$M_C^y = \int_s \omega^2 x_{c0} z_{c0} dm \tag{2}$$

Where, $x_{c0} = |\vec{R}_0| \cos\theta$, $z_{c0} = |\vec{R}_0| \sin\theta + r$.

$\vec{R}_0$ is the projection on xoz plane of the vector of dm barycentric coordinate. And ω is clockwise angular velocity of the hub viewing from the positive x axis direction, and $\omega = 2\pi n / 60$.

Folding propeller can be regarded as a rigid body. Therefore, the quality of the blade may be regarded as focusing on one point of the center of mass C (x_c, y_c, z_c).Equation (2) is converted to:

$$M_C^y = m\omega^2 (R\sin\theta + r) R\cos\theta \tag{3}$$

We continue to transform the above formula as:

$$M_C^y = m\omega^2 R(\frac{R}{2}\sin 2\theta + r\cos\theta) \tag{4}$$

We define the following two functions:

$$f(\omega) = m\omega^2 R \, , \, f(\theta) = \frac{R}{2}\sin 2\theta + r\cos\theta$$

We found that $f'(\omega) = 2m\omega R > 0$ .Therefore the function $f(\omega)$ is an increasing function.

And the derivative of the function $f(\theta)$ is: $f'(\theta) = R\cos 2\theta - r\sin\theta$.

If we let $f'(\theta) > 0$, then we get:

$$0 < \theta < \arcsin\left(\frac{1}{4}\left(\sqrt{\left(\frac{r}{R}\right)^2 + 8} - \frac{r}{R}\right)\right) \tag{5}$$

R is the projection length on xoz plane of the distance between the center of mass C and the origin o .We calculated that $R = 0.0543m$. We obtained $0 < \theta < 41.5°$ by substituting the value of R and r into (5). According to the definition of monotonic, we can get the following conclusions:

a) $f(\theta)$ is increasing if $0 < \theta < 41.5°$.

b) $f(\theta)$ is decreasing if $41.5° < \theta < 90°$.

We found that M_C^y and $f(\theta)$ have the same monotonic at the same ω . Therefore M_C^y increases first then decreases with respect to θ at the same value of ω . Based on (3) and (4), we drew a curve of M_C^y with respect to θ and ω , as shown in Fig. 6.

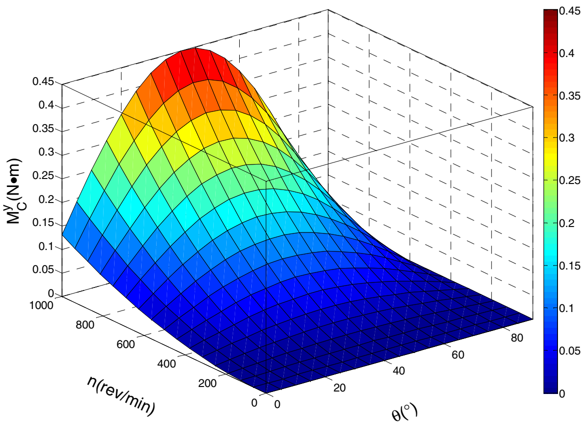

Fig. 6. The curve of M_C^y with respect to θ and ω

Through the curve above we can found that M_C^y indeed agree with the law of increasing first and then decreasing, and we noted that $M_C^y = 0$ at $\theta = 90°$ .Therefore the blade is unable to be fully unfolded with only the blade centrifugal force. We also need the role of hydrodynamic. Therefore we need to study the effect of hydrodynamic moment of the blade.

In (1), M_H^y is the hydrodynamic moment of the blade acting on the y axis with unit $N{\bullet}m$ and can be calculated through the following equations:

$$M_H^y = f(\rho, n, D, J) = K_{M_H} \rho n^2 D^5 \quad (6)$$

$$K_{M_H} = K_0^M + K_1^M J + K_2^M J^2 \quad (7)$$

In (6), ρ is the density of water and should equals to 104.6 $kgf \cdot s^2 / m^4$ in ship theory; n is the rotating speed of the propeller with unit rev/s ; J is the advance coefficient; K_{M_H} is the hydrodynamic moment coefficient; K_0^M , K_1^M , K_2^M all are hydrodynamic coefficients.

M_S^y is the spring torque of the blade acting on the y axis with unit $N{\bullet}m$ and can be calculated by the following formula:

$$M_S^y = \frac{EI\theta}{\pi d_2 N} \quad (8)$$

In the formula above, E is the elastic modulus with unit MP_a ; I is the cross sectional moment of inertia of spring wire with unit mm^4 ,and $I = \pi d_1^4 / 64$; d_1 is the diameter of the spring wire with unit mm ; d_2 is the median diameter of the spring coil with unit mm ; θ is the torsional deformation angle, namely the blade folding angle (see Fig.5(a)) with unit rad , and $0 \le \theta \le \frac{\pi}{2}$; N is the number of spring laps. After putting the above parameter values into (8), we can obtain the following equation:

$$M_S^y = 0.0455\theta \quad (9)$$

M_G^y is the moment of gravity of the blade acting on the y axis with unit $N{\bullet}m$ and can be calculated by the following formula:

$$M_G^y = G\cos\varepsilon x_c \quad (10)$$

In the formula above, G is the gravity for a single blade. ε is the angle between the longitudinal plane and the z axis, and $0^\circ \le \varepsilon \le \pi$. We can obtain $x_c = R\cos\theta$ by the knowledge of geometry. Therefore, (10) can be converted as:

$$M_G^y = mgR\cos\theta\cos\varepsilon = 0.012\cos\theta\cos\varepsilon \quad (11)$$

The curve of M_G^y with respect to θ and ε is shown in Fig.(7).We found that the maximum of M_G^y is : $0.012 N \cdot m$,corresponding with θ =0 and ε =0. Through the above analysis, we found that the maximum of M_G^y occurs at the moment when HDUG is switched from zero velocity or glider mode to AUV mode or mixed mode. In addition, the blade-closed-surface is in the horizontal position shown in Fig.2.

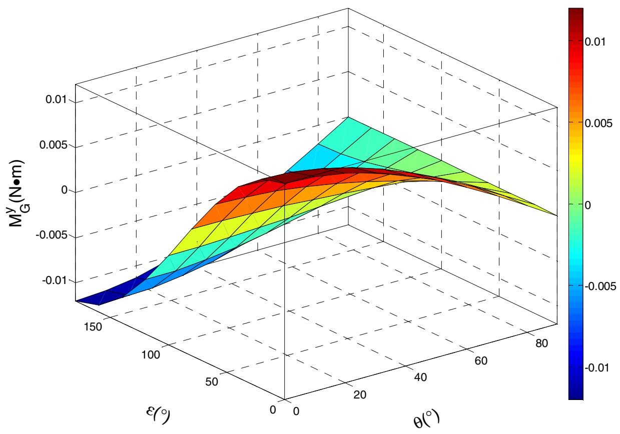

Fig. 7. The curve of M_G^y with respect to θ and ε

Based on the above analysis, in the assumption of n = 600rev/min, (1) can be converted as:

$$\begin{aligned} &-(0.1279\sin 2\theta + 0.0471\cos\theta) - M_H^y \\ &+0.0455\theta + 0.012\cos\theta\cos\varepsilon = 0 \end{aligned} \quad (12)$$

2) Blades Folding

When the HDUG needs to switch to Glider mode, the driven motor stop working, the two blades are folded by the water pressure on the dorsal surface of the blades and the torque spring moment. According to the principle of moment balance, we get:

$$M_D^y + M_S^y - M_G^y = 0 \quad (13)$$

M_D^y is hydrodynamic moment by the fluid acting on the back of the blade with respect to the y axis which can be calculated by CFD method.

III. PROCESS OF CFD CALCULATION

In this paper, we use multiple reference frame (MRF) method to built a fixed fluid domain with respect to a static coordinate system and a rotating fluid domain with respect to a moving coordinate system[18]. The purpose to do this is to simulate a viscous flow field around the propeller at a certain rotation angular in the coming stream. Learning from the experience of numerical calculations, we built the fixed domain by a cuboid space cutting a small internal cylinder space. And the rotating domain is built by the space between the surface of the former cylinder and the internal propeller. The dimension of the cuboid is 8 meters in length, 4 meters in width, and 3 meters in height. The dimension of the cylinder is 0.3 meter in bottom radius and 0.3 meter in height. And we used the software ICEM to mesh grid for the two domains and then put them in one numerical example to simulate by the software CFX. In this paper, we used the following boundary conditions:

- Velocity inlet boundary condition: when the propeller advance coefficient J is not 0, we considered the propeller placing in a fixed location. And the far field upstream direction is defined as the velocity inlet boundary;
- Static pressure outlet boundary conditions: the far field downstream direction is defined as static pressure outlet boundary;
- Free-slip adiabatic wall conditions: we use this to simulate the smooth wall;
- No-slip smooth adiabatic wall condition: we use this to simulate the propeller blades.

IV. Results and Analysis of Open Water Performance Calculation

This paper assumes that the propeller driven motor speed is $n = 600 rev/\min$ .We calculated the hydrodynamic performance of the folding propeller at different folding angles: $\theta = 0 \sim 90^\circ$ and different advance coefficients: $J = 0.1 \sim 0.6$ (corresponding to $V = 0.28 \sim 1.68 m/s$). The calculation models with respect to different θ are shown in Fig.8.

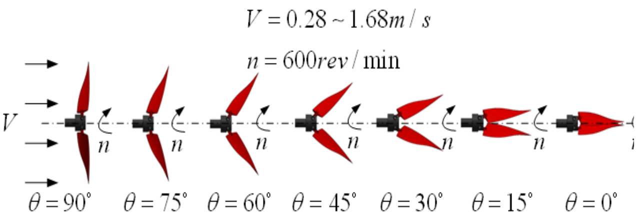

Fig. 8. The calculation models with respect to different θ from $0 \sim 90^\circ$

A. The Hydrodynamic Performance at $\theta = 90^\circ$

First, we calculated the hydrodynamic performance of the folding propeller at $\theta = 90^\circ$ .Then according to (14)-(17)[16], we obtained the thrust coefficient K_T , torque coefficient K_Q , and open water efficiency η of the folding propeller under different advance coefficients J (see Fig.9).

$$K_T = \frac{T}{\rho n^2 D^4} \tag{14}$$

$$10K_Q = \frac{10Q}{\rho n^2 D^5} \tag{15}$$

$$\eta_0 = \frac{J}{2\pi} \cdot \frac{K_T}{K_Q} \tag{16}$$

$$J = \frac{V}{nD} \tag{17}$$

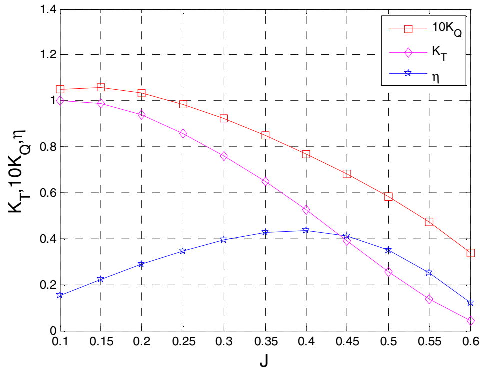

Fig. 9. The curve of open water performance of the folding propeller at $\theta = 90^\circ$

We can find from the figure above that the curve is smooth and regular. The curve of K_T has the same distribution law as the curve of K_Q and bends down with J increasing. Generally people think that the two curves approximate parabolic.

B. The Hydrodynamic Performance at $\theta = 0 \sim 90^\circ$

Through the calculation of hydrodynamic performance under different θ , we can find that the propeller has highest efficiency at $\theta = 90^\circ$, as shown in Fig.10. So in order to obtain the highest thrust performance, we should consider making the blades are in fully unfolded position during the folding propeller design.

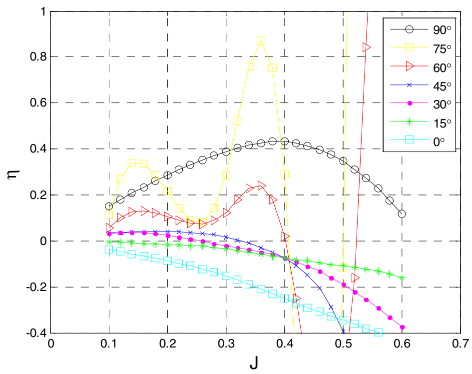

Fig. 10. The open water efficiency under different θ

This paper also simulated M_H^y under different J and different θ to quantitatively analyze the dynamic changing process of the folding propeller. Through (15), we could calculate $K_{M_H}^{y}$ with the curve shown in Fig.11.

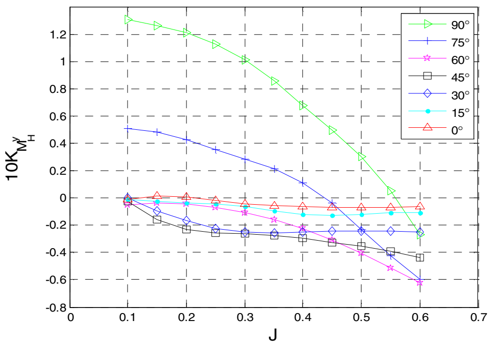

Fig. 11. The value of M_H^y with respect to different J and θ

From the figure above, we found at the same θ, the smaller J, the more $K_{M_H^y}$. So when the speed equals 0, the hydrodynamic moment on the blade reaches to maximum. In this case, it's conducive to open the blades; But at the same J, it is found that $K_{M_H^y}$ is not strictly monotonous with the increasing θ. Therefore, through the above analysis, combined with the actual work mode of HDUG, we got the following conclusions:

- When the HDUG switches from the glider mode to AUV mode, the hydrodynamic moment acting on the blade is minimum, and it is hardest for the propeller unfolding;
- When the HDUG switches from cruising velocity of 0 to AUV / Glider mixed mode, the hydrodynamic moment acting on the blade is maximum, and it is easiest for the propeller unfolding.

Seen from the above conclusion, it is necessary to analyze the case in the HDUG switching from the glider mode to AUV mode. Typically in glider mode, the advance coefficient of the HDUG is J=0.2 (corresponding to $V = 0.56m/s$). We obtained the curve of M_H^y with respect to different θ when J=0.2 shown in Fig.12.

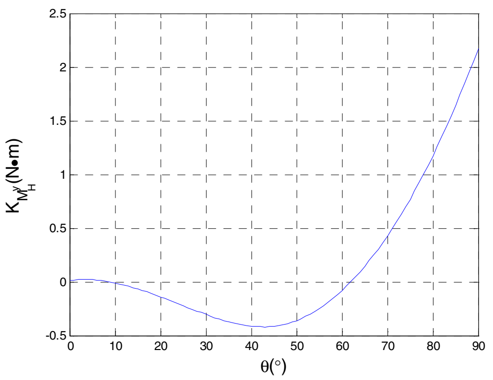

Fig. 12. The curve of M_H^y with respect to different θ when J=0.2

The relationship of M_H^y and θ were fitted as a sixth-order polynomial:

$$M_H^y = 0.011 - 0.1441\theta + 1.1219\theta^2 - 10.2614\theta^3 + 16.9118\theta^4 - 9.8727\theta^5 + 2.0533\theta^6 \tag{18}$$

V. Results and Analysis of Drag

A. Drag Deduction Fraction

To verify the low resistance superiority of the folding propeller better than conventional fixed-wing propeller, we need to simulate the drag performance of the folding propeller. Since the case of towing drag only happens in glider mode, and the velocity of the HDUG in this case is usually slower than 2 knots, the velocity range in the towing experiments simulation is given as $V = 0 \sim 1.4m/s$. The towing experiment has a similar calculation model as the open water experiment's. The only difference is that the towing experiment makes the rotating domain in the open water experiment stationary, namely makes the rotating speed of the driven motor zero.

We use drag deduction fraction τ characterize the low resistance performance of the folding propeller:

$$\tau = \frac{D_U - D_F}{D_U} \tag{19}$$

Here, D_U is the unfolding drag, equaling to the towing drag of the propeller when the blades unfolded. D_F is the folding drag, equaling to the towing drag of the propeller when the blades folded. The model of the propeller in towing experiment is shown in Fig.13.

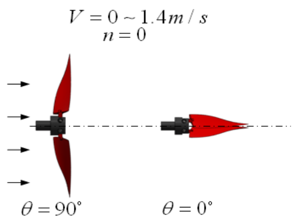

Fig. 13. The calculation model of the propeller in towing experiment

The results of the towing experimental are shown in Fig.14.

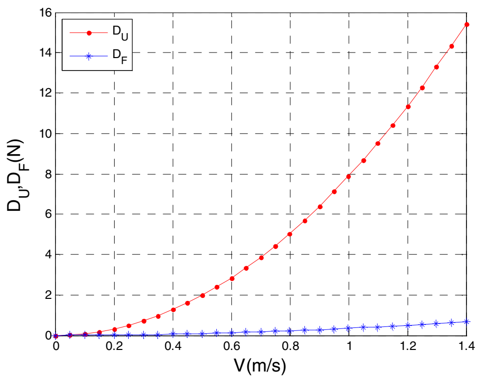

(a) The results of D_U and D_F with respect to different V

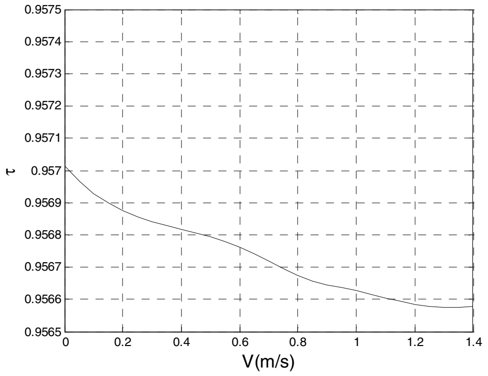

(b)The results of drag deduction fraction τ with respect to different V

Fig. 14. The results of towing experiment of the folding propeller

From the above results, we can find that the drag is significantly reduced from unfolding to folding, a drop of 95% or more, with obvious advantages of low resistance performance.

But for the HDUG, the low resistance performance of the folding propeller performance is reflected in the whole system not in the propeller alone. Therefore, it is necessary to present the drag deduction fraction of the whole system $\tau^{'}$.We defined $\tau^{'}$ as:

$$\tau^{'} = \frac{D_U^{'} - D_F^{'}}{D_U^{'}} \tag{20}$$

$D_U^{'}$ is the unfolding drag, equaling to the towing drag of the HDUG when the blades unfolded. $D_F^{'}$ is the folding drag, equaling to the towing drag of the HDUG when the blades folded. Therefore this paper simulated the towing drag performance of the whole HDUG with respect to the blades of the propeller being in folded and unfolded respectively. In order to ensure accurate calculation, the fluid domain dimension was chosen as: 16m length, 8m width, and 6m height, as shown in Fig.15. Where, the main dimensions of the HDUG model are shown in table 2.

Fig. 15. The fluid domain of integrated system of HDUG

TABLE II. MAJOR DIMENSIONS OF HDUG MODEL

Length of HDUG(m)	2.073
Diameter of HDUG(m)	0.22
Length/diameter ratio of HDUG	9.4
Span of horizontal wing(m)	1
Diameter of propeller(m)	0.28
Height of vertical rudder(m)	0.15

Since the case of towing drag only happens in glider mode, and the velocity of the HDUG in this case is usually slower than 2 knots, the velocity range in the towing experiments simulation of the integrated system of the HDUG is given as $V = 0 \sim 1.0 m/s$.The results are shown in Fig.16.

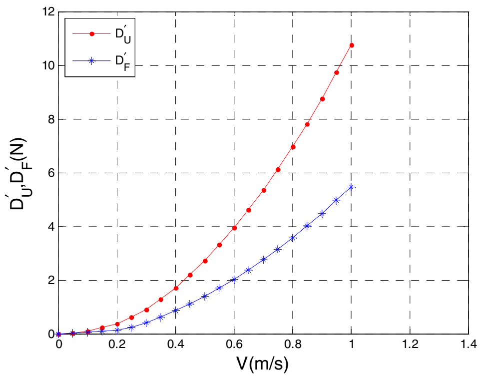

(a) The results of $D_U^{'}$ and $D_F^{'}$ with respect to different V

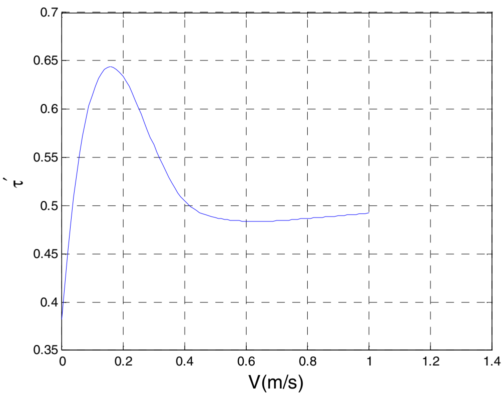

(b)The results of drag deduction fraction $\tau^{'}$ with respect to different V

Fig. 16. The results of towing experiment of the integrated system of the HDUG

From the figures above, we found that the average drag deduction fraction of the whole system $\tau^{'}$ is 45%, and this value can reach to higher than 60% especially at V=0.2m/s .This result is valuable in research and application for HUDG. This shows that the way using the folding propeller instead of traditional fixed-wing propeller to reduce the drag of the HDUG is effective.

B. *Towing Hydrodynamic Moment*

In order to analyze the folding process of the folding propeller, we need to calculate the hydrodynamic drag moment M_D^y .The simulation model is the same as the model of the HDUG's towing experiment with $V = 0 \sim 2m/s$ and $\theta = 0 \sim 90^{\circ}$ (interval 15°).The results are shown in Fig.17.

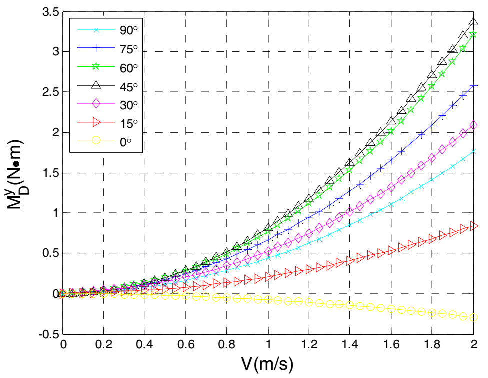

Fig. 17. The value of M_D^y with respect to different V

We can find from the figure above that at the same speed, with θ increasing, M_D^y first increases then decreases, not monotonically increases (see Fig. 18).

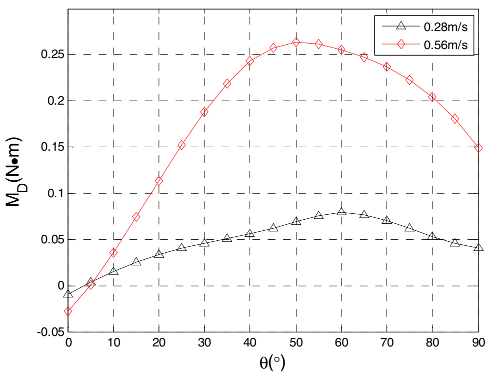

Fig. 18. The value of M_D^y with respect to different θ

Here, we analyze the reasons for this phenomenon. Since the M_D^y generated not only from the forward flow hydrodynamic drag force D, but also from the hydrodynamic lift force L. According wing theory, when the inflow direction is fixed, with the increase of θ, the angle of attack is increased, result in the lift force L increasing. When exceeding the stall angle of attack, the lift begins to decrease. Although in the whole process, the drag force has been showing increasing regularity, as shown in Fig.19, the M_D^y generated by the resultant first increases then decreases as shown in Fig.18. We find from Fig.19 that the stall angle of attack is more or less 50°. That is, when the HDUG switches from AUV mode or mixed mode to glider mode, the maximum hydrodynamic moment occurs not in $\theta = 90°$ but in $\theta = 50°$.

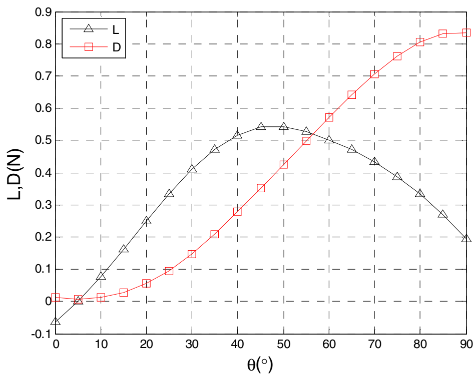

Fig. 19. The value of L and D with respect to different V

VI. Comprehensive Analysis

A. Blades Unfolding

Through the previous studies, we see that when the HDUG switches from glider mode to AUV mode or mixed mode at $n = 600 rev/\min$, (1) must ≤ 0 to make sure the blades fully open namely $\theta = 90°$.

$$-M_H^y - M_C^y + M_S^y + M_G^y \le 0 \tag{21}$$

We converted the equation above to:

$$M_H^y + M_C^y - M_S^y - M_G^y \ge 0$$

By (12) and (18),we obtained:

$$\begin{aligned} M_u^y &= -(0.1279\sin 2\theta + 0.0471\cos\theta) \\ &-(0.011 - 0.1441\theta + 1.1219\theta^2 \\ &-10.2614\theta^3 + 16.9118\theta^4 \\ &-9.8727\theta^5 + 2.0533\theta^6) \\ &+0.0455\theta + 0.012\cos\theta\cos\varepsilon \le 0 \end{aligned}$$

We obtained the curve of the value of M_u^y with respect to different θ as shown in Fig.20.

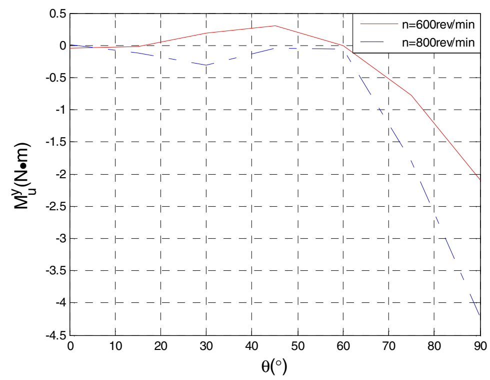

Fig. 20. The curve of M_u^y with respect to different θ

From the above chart, we discovered that the curve of M_u^y has some part in positive area at a rotor speed of $600 rev/\min$. So this result is not we wanted. But when the rotor speed is at $800 rev/\min$, the whole curve of M_u^y is in negative area. This result is what we wanted. This shows that the design of the propeller meets the requirements.

B. Blades Folding

As the same as the analytical method of blades unfolding, considering (13), we obtained the following inequality:

$$M_f^y = -0.01 + 0.054\theta + 0.843\theta^2 - 3\theta^3 + 4.266\theta^4$$
$$-2.697\theta^5 + 0.621\theta^6 + 0.0455\theta - 0.012\cos\theta\cos\varepsilon$$
$$\geq 0$$

We charted a curve of the relationship of M_f^y and θ in Fig.21.

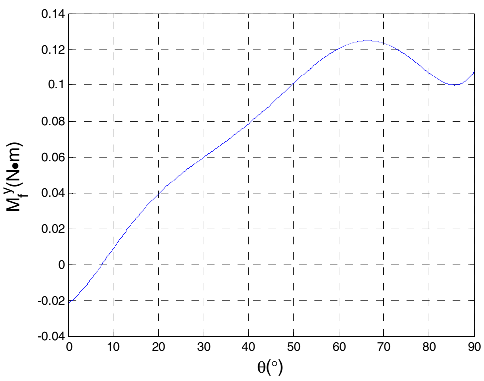

Fig. 21. The curve of M_f^y with respect to different θ

From the above chart, we see that the average of M_f^y is greater than 0 when $\theta > 10°$. That is to say the blades of the designed folding propeller in this paper can be successfully folded in glider mode when $\theta > 10°$.

VII. CONCLUSION

This paper discussed the open water performance and low resistance performance of the folding propeller designed by us. Based on the above results, we compared the performance of the folding propeller device in different working conditions and examined the device designed in this paper if it satisfied the (1) and (2). We found that the design meet the requirements well when the motor speed is greater than 800 revolutions per minute. Furthermore, the resistance deduction τ' of the HDUG is 45% between with folding propeller device and with the conventional fixed-wing propeller device. The value τ' can reached to higher than 60%, especially at the velocity of the HDUG equal to 0.2 meters per second, which is valuable in research and application for HUDG.

ACKNOWLEDGMENT

The authors acknowledge the support of the National Natural Science Foundation of China under Grant 51179183 and the support of the Defense Industrial Technology Development Program of China under Grant B1320110060.

REFERENCES

[1] D. L. Rudnick, R. E. Davis, C. C. Eriksen, D. M. Fratantoni, and M. J. Perry, "Underwater gliders for ocean research," Mar. Technol. Soc. J., vol. 38, p. 12, 2004.

[2] G. Griffiths, C. P. Jones, J. Ferguson, and N. Bose, "UNDERSEA GLIDERS," Ocean Technology, 2007.

[3] R. E. Davis, C. C. Eriksen, and C. P. Jones, "Autonomous Buoyancy-driven Underwater Gliders," The Technology and Applications of Autonomous Underwater Vehicles (AUV), 2002.

[4] X. K. Zhu, J. C. Yu, and X. H. Wang, "Adaptive Coverage Sampling of Underwater Glider," ROBOT, vol. 34, pp. 566-573, 2012.

[5] C. C. Eriksen, T. J. Osse, R. D. Light, T. Wen, T. W. Lehman, P. L. Sabin, et al., "Seaglider: a long-range autonomous underwater vehicle for oceanographic research," IEEE J.Oceanic Engng, vol. 26, p. 13, 2001.

[6] J. Sherman, R. E. Davis, W. B. Owens, and J. Valdes, "The autonomous underwater glider 'Spray'," IEEE J. Oceanic Engng, vol. 26, p. 10, 2001.

[7] D. C. Webb, P. J. Simonetti, and C. P. Jones, "SLOCUM: an underwater glider propelled by environmental energy," IEEE J. Oceanic Engng, vol. 26, p. 6, 2001.

[8] J. C. Yu, A. Q. Zhang, W. M. Jin, Q. Chen, Y. Tian, and C. J. Liu, "Development and Experiments of the Sea-Wing Underwater Glider," China Ocean Eng, vol. 25, pp. 721-736, 2011.

[9] L. M. Merckelbach, R. D. Briggs, D. A. Smeed, and G. Griffiths, "Current measurements from autonomous underwater gliders," in In Proceedings of the Ninth IEEE/OES Working Conference on Current measurement technology, New York, 2008, pp. 61-67.

[10] B. Claus, R. Bachmayer, and C. D. Williams, "Experimental flight stability tests for the horizontal flight mode of a hybrid glider," Autonomous Underwater Vehicles (AUV), 2010.

[11] A. Caffaz, A. Caiti, G. Casalino, and A. Turetta, "The hybrid glider/AUV Folaga," IEEE Robotics Automn Mag, vol. 17, p. 14, 2010.

[12] B. Claus, "Hybrid Glider Propulsion Module Implementation and Characterization," Autonomous Underwater Vehicles (AUV), 2010.

[13] K. Isa and M. R. Arshad, "Neural Networks Control of Hybrid-Driven Underwater Glider," OCEANS, 2012-Yeosu, 2012.

[14] Y. L. Page, "Innovative glider technologies," in In Proceedings of the Third European Gliding Observatories Workshop and Glider School (EGO2008), La Spezia, Italy, 27–31 October 2008.

[15] J. G. Wu, "System Design and Performance Analysis of Hybrid-driven Underwater glider," Doctor, Tianjin University, Tianjin, 2012.

[16] Z. B. Sheng and Y. Z. Liu, Ship Theory. Shanghai: Shanghai Jiaotong University Press, 2004.

[17] S. W. Zhang, J. C. Yu, and A. Q. Zhang, "Optimal control for underwater gliders in the vertical plane," Control Theory & Applications, vol. 29, pp. 19-26, 2012.

[18] A. N. Hayati, S. M. Hashemi, and M. Shams, "A study on the behind-hull performance of marine propellers astern autonomous underwater vehicles at diverse angles of attack," Ocean Engineering, vol. 59, pp. 152-163, 2013.